

Localization and deformation in laponite sand mixtures

Sudhanshu Rathore^{1,*}, Shruti Pandey¹, and Tejas G Murthy^{1,**}

¹Department of Civil Engineering, Indian Institute of Science, CV Raman Rd, Bangalore - 560012, INDIA

Abstract. Presence of small amounts of cohesion or fines in a granular ensemble usually restricts the particle rearrangement and, in effect, changes the ensemble's mechanical response. Plastic fines, such as clay particles present in the sand, impart enhanced ductility. A series of orthogonal cutting experiments were carried out on laponite clay-sand mixtures to understand the effect of the presence of highly plastic fines on the formation of zones or regions of localizations/shear bands. Clay suspension was prepared by dispersing laponite in water, which was further mixed with sands. The sand-laponite mixture was characterized by unconfined compression tests at different loading rates. The laponite provides an interesting interstitial scaffold in the sand particle ensemble, in effect, hindering particle rearrangement in such mixtures via its thixotropic properties. Gelation of the laponite in the pore spaces caused rate-dependent strength enhancement to the model soil. Severe plastic deformation followed by separation of the soil wedge via fracturing was observed as a cyclic mechanism of cutting in sand-laponite. Load response during cutting was observed to be a function of rate and depth.

1 Introduction

Clay minerals are widely used in several industrial processes as oil drilling fluids and as gelling agents. Laponite is one such commercially available clay-like mineral that is widely used as a rheology modifier in numerous applications due to its thixotropic properties. Laponite is a synthetic pure hectorite nano-clay (a type of smectite mineral) that forms a colloidal solution when dispersed in water and swells with time [1].

The presence of small amounts of fines dramatically alters the particle interaction in a granular ensemble, restricting the particle rearrangement at the grain scale while changing the mechanical response at the ensemble scale. Modern materials, such as nanomaterials, fibres, etc., are recently being sought in applications such as liquefaction mitigation, hybrid manufacturing (i.e., 3D printing), and innovative sustainable infrastructure materials (e.g., considering carbon footprint, environmental effects) [2, 3]. In this regard, materials such as bentonite, silica gel, and nano-clays (like Laponite) are gaining prominence in the innovative solutions for soil improvement as being less expensive to the environment and as well as being economical[4].

Past studies highlight the significant influence of small Laponite percentages (1% by weight of sands) on the cyclic resistance, pore pressure development, and small strain dynamic properties of sand-laponite mixtures [1]. Two mechanisms were observed to be attributed to the reduction in particle mobility in Laponite-treated sand - (i) cementation at the sand grain contacts and (ii) gelation of the pore fluid [5]. In a study using the centrifuge model,

[6] reported that the solid-like nature of the Laponite dispersion delayed the excess pore pressure build-up and spread by raising the elastic strain threshold.

While most of the research has examined specific applications of laponite sand as a means for controlling liquefaction, studies exploring the large strain and strain rate response on the deformation properties of these mixtures are few and far between. The orthogonal cutting configuration [7] allows an examination of the operative mechanism of the sand laponite under large deformations with a focus on the influence of laponite on the pore space in a sand ensemble. This paper presents the results of the orthogonal cutting experiments in the model material of laponite-sand (LS) mixtures. The deformation kinematics were investigated through velocity, effective strain rate, and volumetric strain rate fields. Cutting forces were also presented to reveal the possible effects of the rate of cut (cutting speed) and depth of cut.

2 Experimental details

2.1 Materials

Laponite-RD is used as the model viscous binder (gelling agent) to fill the voids of the quartz sand ensemble. Laponite suspensions with 2% laponite by weight of sands are prepared using deionized water, followed by the addition of 1% sodium pyrophosphate (by weight of laponite) solution as a dispersing agent to control the rate of gelation. Minerals present in the Laponite RD are - silicon dioxide (SiO₂), magnesium oxide (MgO), sodium oxide or soda (Na₂O), and lithium oxide (Li₂O) in 65.82%, 30.15%, 3.20%, and 0.83% proportions, respectively [8].

Laponite-sand (LS) material model system was prepared using very angular, semi-elongated quartz sands

*e-mail: sudharsh9597@gmail.com

**e-mail: tejas@iisc.ac.in

as the base material with laponite as the model viscous binder. For the preparation of the LS samples, freshly prepared (with almost zero ageing time) 2% laponite suspensions are used as they exhibit a solution state similar to water, allowing ease in specimen reconstitution. The target density and water content for the saturated LS specimens were 1.5gm/cm³ and 29%, respectively. Further details are presented elsewhere [9]. The homogeneity of the reconstituted sample was examined in order to verify the efficacy of the specimen reconstitution technique. Samples were examined for their spatial distribution of moisture, laponite content, and density.

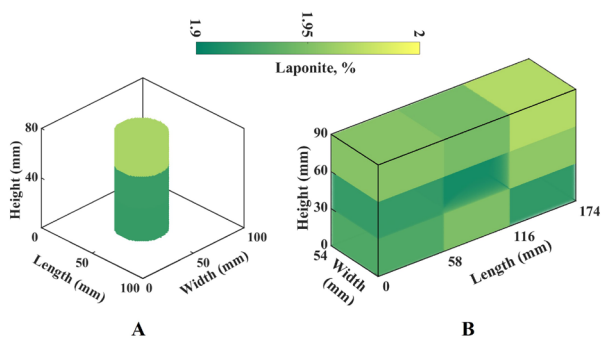


Figure 1: Laponite content across A. UCS sample and B. Cutting sample

Φ38×76 mm sized cylindrical samples for unconfined compressive strength (UCS) tests and the 174mm×90mm×55mm sized cuboid-shaped samples for orthogonal cutting (OC) experiments were prepared. Figure 1 shows the laponite content in different sectioned chunks of samples. It was observed that regardless of the sizes of the specimens prepared, the density, water content, and laponite content were found to be uniform as the mean values were within the 5% error range from target values. [9].

2.2 Methods

The rheological properties of the 2% laponite suspensions were studied in their sol, gel, and sol-to-gel transition states, achieved at different aging times at 25°C are presented in detail elsewhere [9].

Unconfined compression tests were performed on a mini Instron single-column electromechanical testing load frame with a load cell of 200N capacity for an initial characterization of the sand-laponite specimens.

In-plane orthogonal cutting experiments on the saturated LS cuboidal specimens were carried out on a custom-designed CNC machine. The cutting box was fixed on the translation stage of the CNC. A cutting tool was fixed on the dynamometer plate and moved to the required cutting depth inside the box. The LS sample was placed and a glass plate was fitted, ensuring plane strain cutting. The box was moved on the bed of the CNC machine with the region around the fixed tool imaged at high speed and high resolution, and the resulting deformations were computed using particle image velocimetry (PIV) algorithms

[7]. Figure 2 shows the experimental setup for cutting in sand-laponite.

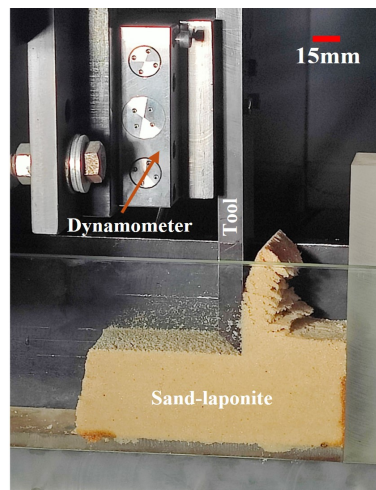


Figure 2: Experimental setup

3 Results & Discussion

A set of sample results from the unconfined compression tests and orthogonal cutting tests is presented in the ensuing. A detailed presentation of the material characterization and orthogonal cutting to investigate rate effects and shear banding is presented in [9].

3.1 Sand-laponite - UCS

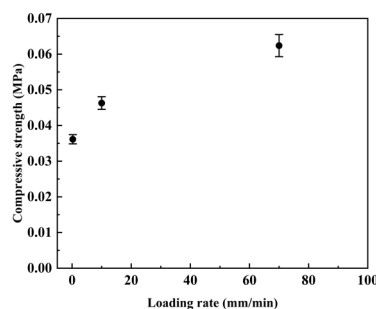


Figure 3: A. Variation of UCS as a function of loading rate

UCS tests of 2% laponite-sand specimens at three different rates of loading - 0.24, 10, and 70mm/min were conducted and the respective strains at peak stresses were found to be around 4.9%, 4.6%, and 3.6% from the stress-strain plots. Figure 3A shows that the mean compressive strengths are 0.036, 0.046, and 0.063 MPa for the three increasing deformation rates. The early peak behaviour, as well as the increased strength and stiffness, showed clear rate-dependency in the mechanical response of the laponite mixed sands.

Preliminary experiments [9] have indicated an increase in the uniaxial compressive strength with curing time -

which can be attributed to the gelation of the viscous pore fluid, thus increasing the pseudo cohesion between the constituent particles.

3.2 Orthogonal cutting in sand-laponite

3.2.1 Deformation field

As the vertical tool starts to drag in the laponite-sand soil, the soil starts to deform. This deformation is the region of retarded velocity vis a vis the bulk as observed through the velocity fields that were obtained from the PIV analysis. Velocity fields during the transient phase were marked with the expansion of the retardation zone (reduced magnitudes of velocity) ahead and below the tool, followed by its contraction. The same is manifested via initial shear strain rate localization that was observed to be spread out significantly in the regions below and in front of the tool. The initial transient phase was found to exist up to a cutting distance equal to the depth of cut, irrespective of depth or speed [9]. Velocity fields in Figure 4(i) indicated multiple flow bifurcation regimes emerging during the cutting of sand-laponite. Dead zones (nearly zero velocity regions) near the tool tip were observed to increase in size with the progression of cutting and with an increase in the initial depth of the cut. Velocity magnitudes within the accumulated pile were found to achieve values as high as the imposed cutting speed (v_c).

Two clear regions of deformation localization were observed in these cutting experiments. In these effective strain rate maps (calculation of the effective strain rate is presented in [7]), regions of high effective strain rate can be considered as a “shear band”. These primary shear bands were observed to emerge from the tooltip, reaching the free surface. In addition to these (primary) shear bands, significant shearing was also frequently observed in the accumulated chip wherein the soil wedge was sliding over a failure surface or fracture plane. It was also observed that the formation of shear bands was more pronounced in the case of higher depth. The formation of shear bands, followed by chipping out of material via shear fracturing mode, occurred cyclically during the cutting.

The volumetric strain rate field (also computed as the sum of the principal strain rates - presented in [9]) was also computed during the deformation. Dilation (or increase in the value of volumetric strain) was seen – in the regions of the primary and secondary shear bands - in effect showing clear material separation. The soil below this secondary shear band is observed to be undergoing significant compaction (i.e., reduction in volumetric strain).

3.2.2 Effect of rate and depth in forces

The resultant cutting forces (F_c) were measured during the cutting tests. At the initiation of cutting, the cutting forces begin to increase (mostly linearly) with the tool displacement, and the initial force peaks at the end of the respective transient phase.

As shown in Figure 5, cutting forces are seen to effectively increase with the tool displacement. This is due to

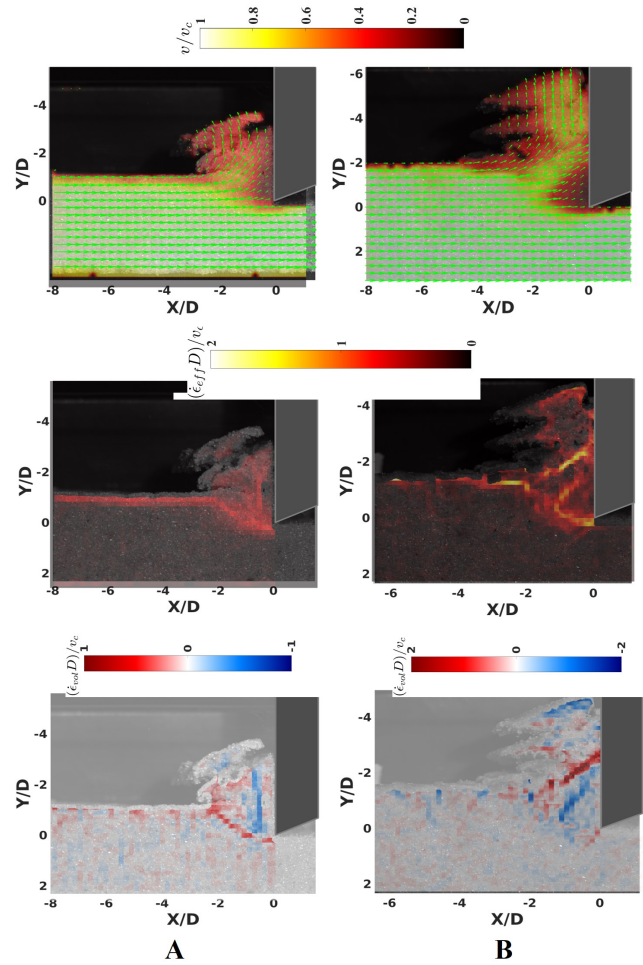


Figure 4: (i) Velocity, (ii) Effective strain rate, (iii) Volume strain rate fields at speed-depth-traverse of A. 10mm/min - 10mm - 42.8mm and B. 1000mm/min - 15mm - 77.3mm

the complex interplay of material compaction, increased effective stresses due to dilation along the shear bands, and hence an increase in failure surface extent. The typical characteristic feature of the force evolution was the periodic occurrence of a peak followed by a significant drop. Coincident with the peaks of the magnitude of the force, a wedge of material begins to separate out from the bulk with continued shearing, i.e., a Mode II type fracture mechanism can be observed, and the fracture plane initiates at the free surface of the sample. The emergence of an incipient shear band in the undisturbed material ahead of the tool was seen coincident with the instance of force drop.

At a lower depth of 10mm, cutting forces were observed to remain almost unchanged to the increase in cutting speeds (by almost 4 orders) up to 50mm (or 5D) cutting distance (region up to PQ in Fig. 5A). With continued cutting and accumulating a sufficient volume of material, the force peak-drop behaviour was significant. The effect of cutting speed was far more pronounced after a certain amount of material was cut (i.e., after about 50mm of cutting was completed). Figures 5A-B show that, for the higher cutting depth of 15mm, the oscilla-

tions in the magnitude of the force are far more apparent. Further, increasing the speed of cutting from 1mm/min to 5000mm/min also shows a significantly higher magnitude of cutting force.

When the cutting force magnitude is examined as a function of cutting depth, presented in Figure 5C-D, increasing depths of cut also increase the cutting force magnitude. Moreover, this depth effect was more pronounced for the higher cutting speeds.

Overall, it is evident that the viscous binder plays a crucial role in facilitating fractures, which result in serrated chips along with significant plastic deformation accompanied by volume change. The rate sensitivity of this fluid also renders the material highly responsive to deformation rates, distinguishing it from typical sands and cemented sands, as highlighted in [9]. As deformation progresses, it becomes localized, leading to the emergence of dilative and contractive bands within the material. This research has opened entirely new questions about how small amounts of fine-grained materials influence the overall dynamics of the response of a granular ensemble. This becomes especially critical in applications including ground improvement and 3D printing of infrastructure elements, where precise material control is vital.

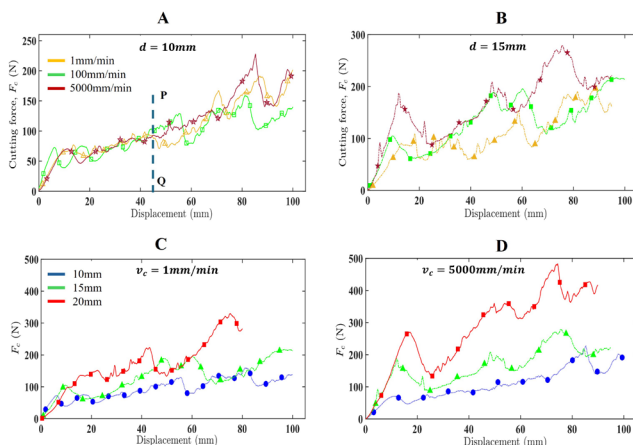


Figure 5: Cutting force evolution at depths - A. 10mm, B. 15mm, and at speeds - C. 1mm/min, D. 5000mm/min

4 Summary

- Orthogonal cutting brings forth an interesting expansion and subsequent contraction of the retardation region and of the intense strain localization in the soil ahead and below the tool during the initial transient phase of cutting.
- At the steady state of cutting, the deformation field is heterogeneous with localized zones of deformation. With the addition of a viscous binder such as laponite to sand, deformation occurs along localized zones (i.e., shear bands) which are also regions of significant volume change. Additionally, fractures occur in the soil as it moves up the rake face of the tool, indicating the formation of chips (as is typically seen in hardening materials such as annealed copper).

- Dilation was observed at the shear bands formed within the material at the localization regions demarcating the separation of the soil wedge at the free surface. Cutting forces effectively increase with the displacement, with the periodic occurrence of peaks and drops in their evolution during cutting. The peak indicated the significant compaction of the soil near the tool and above the shear band, while the drop indicated a mobilization of new shear bands within the soil. The decrease in pore pressure due to dilation in shear bands causes an effective increase in the forces with the traverse distance. Rate effects were dominant in the force responses after only a sufficient volume of material was ploughed.

References

- [1] A. Getchell, F. Ochoa-Cornejo, M. Santagata, Behavior of dry-mixed and permeated laponite-treated sand: from small strains to critical state, *Geotechnical and Geological Engineering* **40**, 5307 (2022). [10.1007/s10706-022-02216-4](https://doi.org/10.1007/s10706-022-02216-4)
- [2] A. Fraccica, G. Spagnoli, E. Romero, M. Arroyo, R. Gómez, Exploring the mechanical response of low-carbon soil improvement mixtures, *Canadian Geotechnical Journal* **59**, 726 (2022). [10.1139/cgj-2021-0087](https://doi.org/10.1139/cgj-2021-0087)
- [3] M. Sharma, N. Satyam, K.R. Reddy, State of the art review of emerging and biogeotechnical methods for liquefaction mitigation in sands, *Journal of Hazardous, Toxic, and Radioactive Waste* **25**, 03120002 (2021). [10.1061/\(ASCE\)HZ.2153-5515.0000557](https://doi.org/10.1061/(ASCE)HZ.2153-5515.0000557)
- [4] G. Liu, C. Zhang, M. Zhao, W. Guo, Q. Luo, Comparison of nanomaterials with other unconventional materials used as additives for soil improvement in the context of sustainable development: a review, *Nanomaterials* **11**, 15 (2020). [10.3390/nano11010015](https://doi.org/10.3390/nano11010015)
- [5] Y. Huang, L. Wang, Laboratory investigation of liquefaction mitigation in silty sand using nanoparticles, *Engineering Geology* **204**, 23 (2016). [10.1016/j.enggeo.2016.01.015](https://doi.org/10.1016/j.enggeo.2016.01.015)
- [6] Y. Huang, Z. Wen, L. Wang, C. Zhu, Centrifuge testing of liquefaction mitigation effectiveness on sand foundations treated with nanoparticles, *Engineering Geology* **249**, 249 (2019). [10.1016/j.enggeo.2019.01.005](https://doi.org/10.1016/j.enggeo.2019.01.005)
- [7] S. Rathore, A. Hegde, T.G. Murthy, Understanding shear bands in granular media through in-plane ploughing experiments at different strain rates, *Granular Matter* **27**, 1 (2025). [10.1007/s10035-024-01489-1](https://doi.org/10.1007/s10035-024-01489-1)
- [8] P. Levitz, E. Lecolier, A. Mourchid, A. Delville, S. Lyonnard, Liquid-solid transition of laponite suspensions at very low ionic strength: Long-range electrostatic stabilisation of anisotropic colloids, *Europhysics Letters* **49**, 672 (2000). [10.1209/epl/i2000-00203-9](https://doi.org/10.1209/epl/i2000-00203-9)
- [9] S. Rathore, Ph.D. thesis, Indian Institute of Science (2025, Unpublished)